

SDSS 1355+0856: A detached white dwarf + M star binary in the period gap discovered by the SWARMS survey ^{*}.

Carles Badenes^{1†}, Marten H. van Kerkwijk², Mukremin Kilic³, Steven J. Bickerton⁴, Tsevi Mazeh⁵, Fergal Mullally⁶, Lev Tal-Or⁵, Susan E. Thompson⁶

¹ *Department of Physics and Astronomy and Pittsburgh Particle Physics, Astrophysics and Cosmology Center (PITT PACC), University of Pittsburgh, 3941 O'Hara St, Pittsburgh PA 15260, USA*

² *Department of Astronomy and Astrophysics, University of Toronto, 50 St. George Street, Toronto, ON M5S 3H4, Canada.*

³ *Homer L. Dodge Department of Physics and Astronomy, University of Oklahoma, 440 W. Brooks St., Norman, OK, 73019, USA*

⁴ *Institute for the Physics of Mathematics of the Universe (IPMU), The University of Tokyo, Chiba 277-8582, Japan*

⁵ *School of Physics and Astronomy, Tel-Aviv University, Tel-Aviv 69978, Israel*

⁶ *SETI Institute/NASA Ames Research Center, Moffett Field, CA 94035, USA*

Accepted 0000. Received 0000; in original form 0000

ABSTRACT

SDSS 1355+0856 was identified as a hot white dwarf (WD) with a binary companion from time-resolved SDSS spectroscopy as part of the ongoing SWARMS survey. Follow-up observations with the ARC 3.5m telescope and the MMT revealed weak emission lines in the central cores of the Balmer absorption lines during some phases of the orbit, but no line emission during other phases. This can be explained if SDSS 1355+0856 is a detached WD+M dwarf binary similar to GD 448, where one of the hemispheres of the low-mass companion is irradiated by the proximity of the hot white dwarf. Based on the available data, we derive a period of 0.11438 ± 0.00006 days, a primary mass of $0.46 \pm 0.01 M_{\odot}$, a secondary mass between 0.083 and $0.097 M_{\odot}$, and an inclination larger than 57° . This makes SDSS 1355+0856 one of the shortest period post-common envelope WD+M dwarf binaries known, and one of only a few where the primary is likely a He-core white dwarf, which has interesting implications for our understanding of common envelope evolution and the phenomenology of cataclysmic variables. The short cooling time of the WD (25 Myr) implies that the system emerged from the common envelope phase with a period very similar to what we observe today, and was born in the period gap of cataclysmic variables.

Key words: binaries: close – binaries: spectroscopic - stars: individual: SDSS 1355+0856– white dwarfs.

1 INTRODUCTION

The common envelope (CE) phase remains one of the key open issues in stellar evolution. Several important classes of astrophysical sources go through at least one CE phase at some point in their lifetime, including cataclysmic variables (CVs), low mass X-ray binaries, detached binary white dwarfs (WDs), AM CVn stars, and very likely the not-yet-identified progenitors of Type Ia supernovae (SN Ia). During the CE phase, the two components of a binary system come into contact and create a shared atmosphere that is ejected

through friction, leading to a loss of energy and a drastic reduction of the orbital period (Paczynski 1976). Due to the challenges involved in performing accurate numerical simulations of the CE phase (Taam & Sandquist 2000; Ricker & Taam 2012), theoretical studies have been largely restricted to simplified analytic calculations. One prescription that has gained wide acceptance is the so-called α formalism, where the eponymous parameter represents the fraction of the orbital energy loss that is consumed in unbinding the common envelope (see Webbink 2006, for a review), but even the fundamental aspects of this prescription are still being revised (see Ivanova & Chaichenets 2011; De Marco et al. 2011; Zorotovic et al. 2011b; Davis et al. 2012).

The most useful constraints on CE evolution come from statistical studies of the properties of post-CE binaries: peri-

^{*} Observations reported here were obtained at the MMT Observatory, a joint facility of the Smithsonian Institution and the University of Arizona

[†] E-mail: badenes@pitt.edu

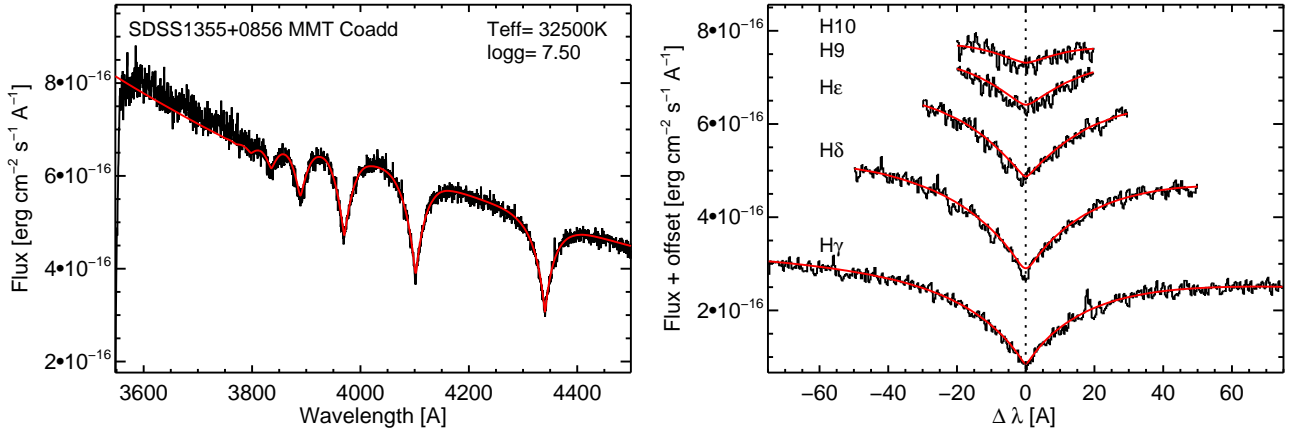


Figure 1. Co-added MMT spectrum of SDSS 1355+0856, together with the best-fit atmosphere model ($T_{\text{eff}} = 32500$ K, $\log g = 7.50$).

ods, mass ratios, and demographics. Zorotovic et al. (2010) compiled a sample of all post-CE WD+main sequence star binaries (WDMS) known at the time: 35 from the SDSS catalogue of Rebassa-Mansergas et al. (2010) plus 25 from the literature, with periods ranging between 0.08 and 21.72 days. Zorotovic et al. found that the properties of these 60 binaries can be explained by the classical α formalism, with α between 0.2 and 0.3 (but see De Marco et al. 2011, for a different analysis based on a smaller sample of systems). In this context, post-CE systems with exceptionally high or low values of the period and/or the masses of the components are especially interesting, because they can test the limits of the CE prescription and put important constraints on the initial and final conditions of CE evolution. Post-CE binaries containing a He core WD ($M \lesssim 0.48 M_{\odot}$; Sweigart & Gross 1978) are of particular interest, because they anchor the low values of α (Zorotovic et al. 2011a), and they have shorter periods and less massive secondaries than their C/O core WD counterparts (Zorotovic et al. 2011b). The final fate of these systems is also puzzling, because few, if any, CVs are known to have a He core WD primary, suggesting they might evolve into classical novae with exceptionally rare outbursts (Shen et al. 2009).

In this paper, we report on SDSS J135523.92 + 085645.4 (henceforth SDSS 1355+0856), a short-period WD binary discovered by the SWARMS survey. SWARMS (Badenes et al. 2009; Mullally et al. 2009; Badenes & Maoz 2012; Maoz et al. 2012) exploits the time-resolved dimension in the spectroscopic database of the Sloan Digital Sky Survey (SDSS) to identify short period double WD binaries (see Bickerton et al. 2012, for a brief summary of the time resolved spectroscopy capabilities in SDSS). SDSS 1355+0856 was originally targeted for follow-up because it fulfilled the SWARMS selection criteria: evidence for radial velocity (RV) shifts between the sub-exposures in the SDSS data and absence of features in the red part of the spectrum that might be associated with a non-degenerate companion (see Section 2). Follow-up observations with the ARC 3.5m telescope and the MMT, however, revealed the presence of weak emission peaks in the Balmer cores of the spectral primary, indicating that the companion is not another WD, but a nondegenerate object. The fact that these emission features are only present at certain orbital phases can be understood

if they originate in the irradiated side of the nondegenerate companion, a behaviour that has been previously noted in systems like GD 448 (also known as WD 0710+741 and LP 034-185 Marsh & Duck 1996; Maxted et al. 1998). From our follow-up observations (Section 3), we derive a period of 0.11438 days for SDSS 1355+0856, placing it in the ‘period gap’ seen in the distribution of CVs, and making it one of the shortest-period post-CE binaries known. In Section 4, we derive estimates for the masses of the components and the orbital inclination, and we discuss the origin and final fate of the system.

2 OBSERVATIONS

2.1 SDSS and selection as a SWARMS candidate

In the DR7 SDSS WD catalogue (Kleinman et al. 2009), SDSS 1355+0856 is classified as an isolated DA WD with $T_{\text{eff}} = 33158 \pm 175$ K and $\log g = 7.37 \pm 0.04$. To verify the basic properties of the WD, we performed an independent fit to a high S/N co-added spectrum obtained after removing RV shifts from the MMT exposures without detected line emission (see Table 2 and Section 3 for details) using the latest version of the DA WD atmosphere models by Detlev Koester (Finley et al. 1997; Koester 2010). Our fitted parameters are close to those of Kleinman et al.: $T_{\text{eff}} = 32500 \pm 250$ K and $\log g = 7.44 \pm 0.05$ (see Figure 1). The system was identified as a candidate short-period binary by the SWARMS survey from the large RV shifts (roughly a hundred km s^{-1}) found between the four SDSS sub-exposures, which were taken with a temporal baseline of three days.

Because SWARMS often detects significant RV shifts from known WDMS binaries, we routinely cross-check all our candidate binaries against the SDSS WDMS catalogue¹ of Rebassa-Mansergas et al. (2012) and remove any matches from our follow-up schedule to maximize the efficiency in our discovery of short-period double WD systems. SDSS 1355+0856, however does not appear in the SDSS WDMS catalogue. Rebassa-Mansergas et al. (2010) describe the procedure they follow to identify WDMS binaries among

¹ Available on-line at <http://sdss-wdms.org>

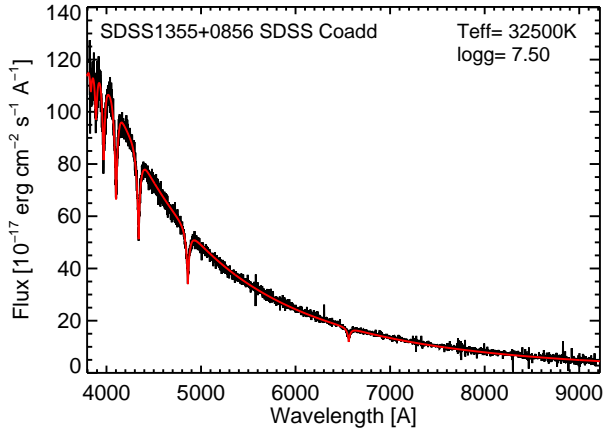


Figure 2. SDSS spectrum of SDSS 1355+0856, together with the best-fit atmosphere model ($T_{\text{eff}} = 32500$ K, $\log g = 7.50$).

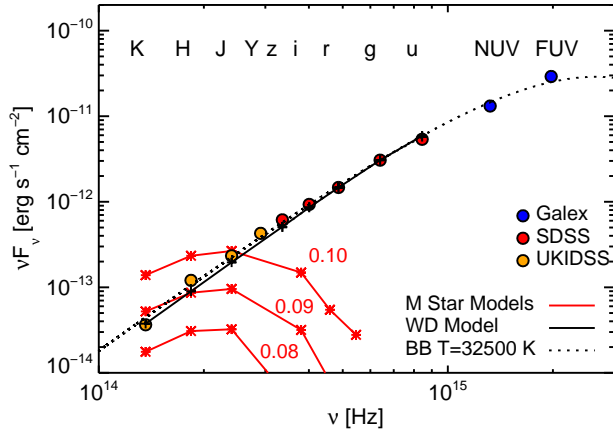


Figure 3. Spectral energy distribution for SDSS 1355+0856. The dotted black line is a blackbody spectrum with $T = 32500$ K, normalized to match the observed flux in the g band. The solid black line is a WD model from Holberg et al. (2006), with $T_{\text{eff}} = 35000$ K, $\log g = 7.5$, and the same normalization. The solid red lines represent low-mass star models from Baraffe et al. (1998), labeled by mass in M_{\odot} .

the SDSS spectra. A key ingredient is the fitting of all candidate objects with WD atmosphere models: any spectra that are well-fit by a WD model in the blue but not in the red are potential WDMS binaries. Rebassa-Mansergas et al. (2010) calculate the χ^2 in the red (7000 to 9000 Å) and in the blue (4000 to 7000 Å), and flag any spectra with $\chi_r^2/\chi_b^2 > 1.5$ as WDMS binary candidates, which are then confirmed based on their infrared photometry. As seen in Figure 2, a single-component WD model provides an excellent fit to the SDSS spectrum of SDSS 1355+0856 in the red - in fact, $\chi_r^2/\chi_b^2 = 0.74$. This explains why the system is not listed in the SDSS WDMS catalogue. For obvious reasons, it is hard to constrain the presence of low-mass M-type companions with hot WD primaries; see Figure 9 of Rebassa-Mansergas et al. (2010) and the accompanying discussion for more details.

In addition to the SDSS broadband photometry, SDSS 1355+0856 has NUV and FUV fluxes from *Galex* (Morrissey et al. 2007) and Y , J , H , and K IR photome-

Table 1. Observational Properties of SDSS 1355+0856

Parameter	Value
R.A. (J2000)	13h 55m 23.92s
Decl. (J2000)	+8° 56' 45.4''
SED (GALEX/SDSS/UKIDSS)	
<i>FUV</i>	1487 ± 60 μJy
<i>NUV</i>	971 ± 27 μJy
<i>u</i>	17.05 ± 0.01 mag
<i>g</i>	17.29 ± 0.01 mag
<i>r</i>	17.76 ± 0.02 mag
<i>i</i>	18.03 ± 0.02 mag
<i>z</i>	18.26 ± 0.03 mag
<i>Y</i>	17.85 ± 0.02 mag
<i>J</i>	17.99 ± 0.04 mag
<i>H</i>	17.98 ± 0.07 mag
<i>K</i>	18.43 ± 0.15 mag
Spectral Parameters (MMT)	
T_{eff}	32050 ± 350 K
$\log g$	7.44 ± 0.05
Orbital Parameters (MMT)	
P	0.11438 ± 0.00006 days
T_0	55275.9613 ± 0.0012 MJD (bar)
K_a	64 ± 8 km s ⁻¹
γ_a	-23 ± 5 km s ⁻¹
K_e	-261 ± 13 km s ⁻¹
$\Delta\gamma_{e-a}$	-4 ± 18 km s ⁻¹
Derived Parameters	
M_1	0.46 ± 0.01 M_{\odot}
M_2	0.083 ≤ M_2 ≤ 0.097 M_{\odot}
i	≥ 57°
$t_{\text{Cool,WD}}$	25 Myr

try from UKIDSS (Lawrence et al. 2007, see Table 1). The broadband SED is reasonably well fit by a blackbody spectrum with $T = 32500$ K, although the measured fluxes in the red and near IR present small deviations with respect to the best isolated WD model in the grid of Holberg & Bergeron (2006) ($T_{\text{eff}} = 35000$ K, $\log g = 7.5$, see Figure 3). When the WD model is normalized to match the measured g flux, the SED of SDSS 1355+0856 is brighter than the model by ~ 0.15 mag in z and J , and ~ 0.3 mag in H . It is hard to explain this flux excess as the contribution of a low-mass stellar companion, because the WD model does match the flux in the K band. A possible explanation for the excess is that the IR data points were taken at different orbital phases, and that the excess in J and H comes from the irradiated side of the companion, but given the known issues with the accuracy of UKIDSS photometry for objects fainter than ~ 18 mag (see e.g. Leggett et al. 2011), the excess might also be purely instrumental.

2.2 Spectroscopic Follow-Up

We observed SDSS 1355+0856 with the Dual Imaging Spectrograph on the 3.5m Astrophysical Research Consortium telescope at Apache Point Observatory on February 9 and 14, 2010. Variable cloud coverage and pointing issues due

to strong winds resulted in extremely noisy spectra. Clear RV shifts were apparent in some spectra, but in other cases the line cores had strange shapes, probably because of inadequate pointing, and the RVs could not be determined with confidence. Because of these issues, we revisited SDSS 1355+0856 with the 6.5m Multiple Mirror Telescope (MMT) at Mt. Hopkins observatory. We used the Blue Channel Spectrograph to obtain moderate resolution spectroscopy of SDSS 1355+0856 on March 19 and 21, 2010. We operated the spectrograph with the 832 line mm^{-1} grating in second order and a $1''$ slit, providing wavelength coverage 3600 Å to 4500 Å and a spectral resolution of 1.0 Å. We obtained all observations at the parallactic angle, with a comparison lamp exposure paired with every observation. We flux-calibrated using blue spectrophotometric standards (Massey et al. 1988). Our observing and reduction procedures were similar to the ones described in Kilic et al. (2010). The superior quality of the MMT data revealed weak but clear emission lines in some of the spectra, but no evidence of line emission in others (see Figure 4).

3 ANALYSIS

The behaviour of the line emission revealed by the MMT data and shown on Figure 4 implies that the companion of SDSS 1355+0856 cannot be a degenerate object, and is probably a faint main sequence star or a brown dwarf. The absence of line emission in some of the spectra can be understood if the system is a binary similar to GD 448 (Marsh & Duck 1996), where one hemisphere of the low-mass main sequence companion is irradiated by the proximity of the hot WD. This results in line emission only during the phases in which most of the irradiated side of the secondary is visible, i.e. when the RV of the primary is increasing between its minimum and its maximum values. In this scenario, the secondary would not contribute much flux to the red part of the SDSS spectrum (Figure 2), especially if most or all of the SDSS sub-exposures were taken during phases in which the irradiated hemisphere was not facing the observer.

To verify the irradiated companion hypothesis, we fitted all the MMT spectra with a two-component model consisting of the best-fit WD atmosphere model from the Koester grid (absorption component), and a set of six equal-strength Gaussian lines in the Balmer series, from H γ to H10 (emission component). For these fits, we scanned over possible RVs v_a and v_e for the absorption and emission components, respectively. For each pair of RV values we fitted for the emission to absorption flux ratio, F_e/F_a (forced to be positive), as well as an overall normalisation, described as a third-order polynomial in wavelength. We then determined the best-fit values of the RVs and their uncertainties by a parabolic fit to the χ^2 surface around the best-fit location, taking F_e/F_a and its uncertainty from the fit to the nearest grid point. For all spectra, we found good fits, with reduced χ^2 values around 0.8. The resulting values are listed in Table 2, where we have corrected all times and radial velocities to the barycenter of the Solar System.

In seven of the 19 spectra (MMT 5, 6, 7, 8, 12, 13, and 18; used to construct the spectrum in Fig. 1), our procedure did not detect any line emission: at the best-fit v_a , the

addition of an emission component made for a worse fit at any value of v_e . Since random chance should lead to some non-zero contributions from the emission component even in spectra that can be described by the absorption component alone, we inspected these fits more closely. We concluded that the absence of spurious detections of an emission component even at unreasonable values of v_e results from our best-fit WD model slightly underpredicting the depths of the line cores (see Fig. 1), so that the best-fit emission component would have a negative flux, which our fit routine does not allow. This is a minor effect that we did not try to correct for, but we note that it implies that our F_e/F_a flux ratios are slightly biased towards low values.

For the spectra with clear emission (MMT 1, 2, 3, 4, 9, 10, 11, 14, 15, 16, and 17), we find that the strength of the emission lines varies quite a bit, with the lines appearing stronger at superior conjunction of the companion (see Figure 4 for an illustration of this variation in the case of H γ - other lines show similar behaviour). The overlap between the cores of the emission and absorption lines makes the determination of the component RVs somewhat challenging, which results in measurements that are more noisy than would be expected in a single-lined system with spectra of similar quality.

We used the RVs to derive orbital solutions of the form $v = \gamma + K \sin 2\pi(t - T_0)/P$ for each component. To get the best possible constraints on the binary period, we fitted the emission and absorption RVs jointly, assuming that they have the same period and anomaly, but are in antiphase. In our procedure, we scan a grid in period, at each point fitting for T_0 , the semi-amplitude of the absorption component K_a , its systemic velocity γ_a , the semi-amplitude of the emission component K_e , and the difference in systemic velocity $\Delta\gamma = \gamma_e - \gamma_a$. Our best-fit orbital solution, shown in Figure 5, has a reduced χ^2 of 1.97 (for 25 d.o.f.), i.e. it is formally not acceptable. This is likely due to inaccuracies of the spectral model. Since the residuals had no obvious phase dependencies, we compensated for the poor quality of the fit by increasing all errors by $\sqrt{1.97}$. We find a period of 0.11438 ± 0.00006 d and epoch of mean longitude $T_0 = 55275.9613 \pm 0.0012$ MJD (barycentric). The small error bar on the period results from fitting absorption and emission jointly, as can be seen from the narrow χ^2 minima in the periodogramme (see Figure 6). However, we can only exclude the alias at 0.12112 d at the 2σ level (the two fits differ by $\Delta\chi^2 = 3.8$). For the best-fit period, we infer $K_a = 64 \pm 8$ km s^{-1} and $K_e = -261 \pm 13$ km s^{-1} for the absorption and emission components, respectively. The systemic velocity for the absorption component is $\gamma_a = -23 \pm 5$ km s^{-1} , and that for the emission component identical within the uncertainties, $\Delta\gamma = -4 \pm 18$ km s^{-1} .

This orbital solution nicely confirms the irradiated companion hypothesis. The spectra without detected line emission are only found between phases 0.25 and 0.75, in the part of the orbit where the RV of the absorption component is decreasing and the irradiated side of the companion is partially or totally occulted by the rest of the star. Outside of this phase range, a larger fraction of the irradiated side of the companion is in view, and the line emission can be easily detected. This scenario makes a specific prediction about the strength of the line emission, which should

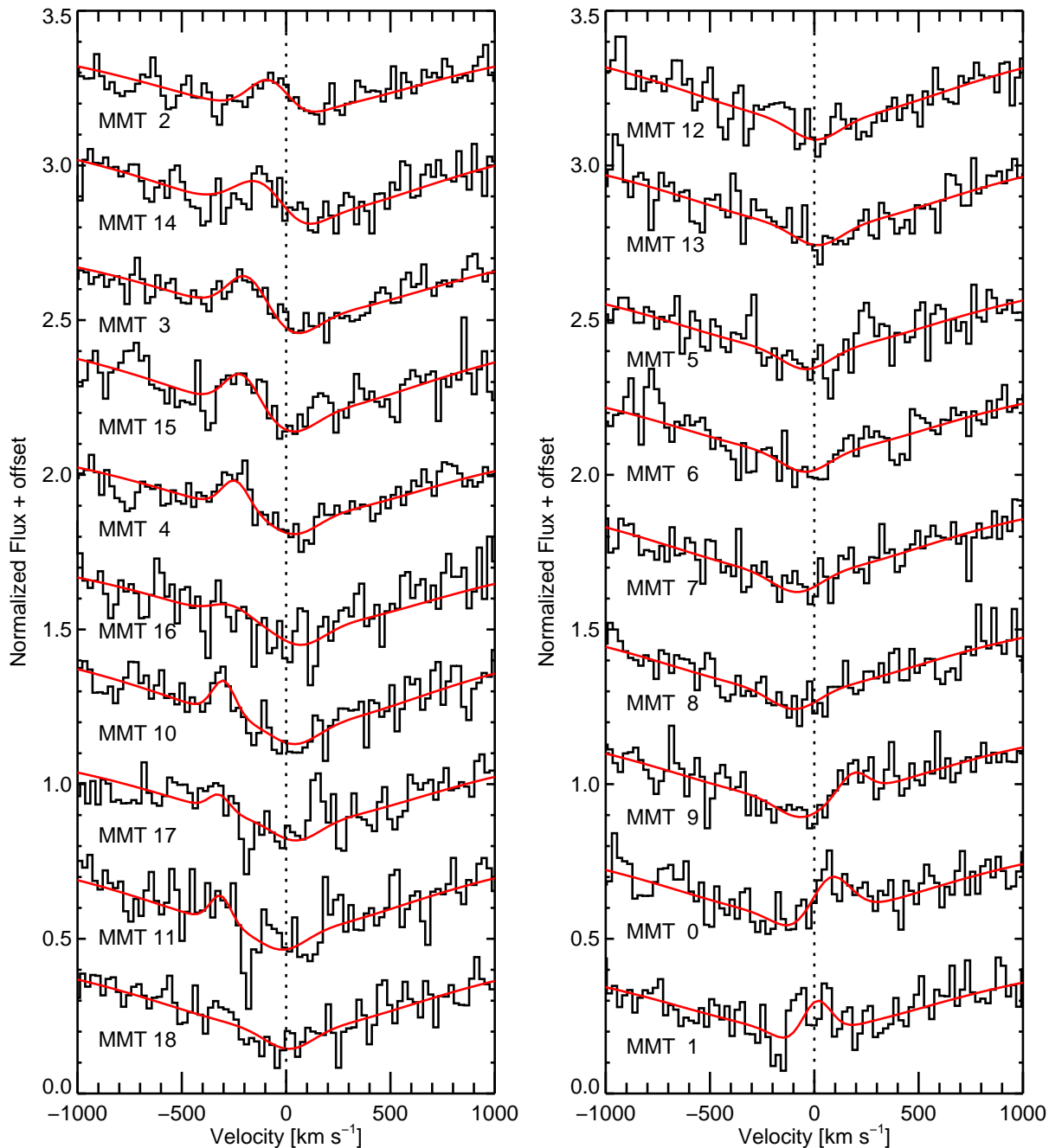


Figure 4. MMT spectra of SDSS 1355+0856 around the $H\gamma$ line, ordered by phase (top to bottom and left to right). No line emission was detected in spectra MMT 18, 12, 13, 5, 6, 7, and 8. The red line is our best-fit model (see Section 3 for details).

peak around phase 0, fall down gradually as the system approaches quadrature (phase 0.25), stay low until quadrature is reached again (phase 0.75), and then increase again. This is indeed the behaviour of the F_e/F_a ratio in the MMT spectra of SDSS 1355+0856 when it is folded through the best-fit orbital solution (see Figure 7). The numerical value of this ratio is arbitrary, because it depends on the normalization of the emission and absorption models that we used to fit the spectra, but qualitatively its orbital evolution matches that of the equivalent width in the line emission of GD 448 (Marsh & Duck 1996; Maxted et al. 1998). For GD 448, the equivalent widths of the emission lines do not go to zero be-

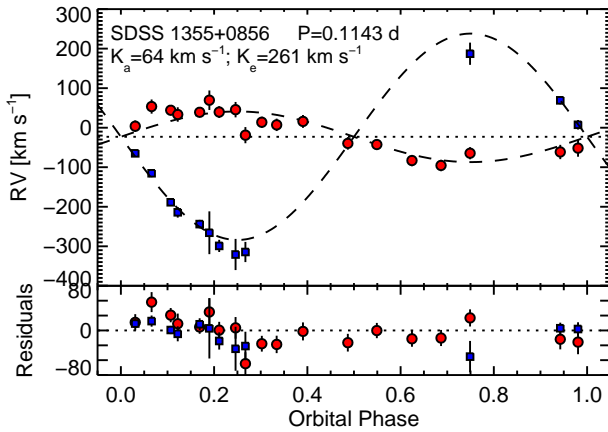
tween phases 0.25 and 0.75, but that is expected given the relatively low orbital inclination of the system ($29.3^\circ \pm 0.7^\circ$ Maxted et al. 1998). The absence of detectable line emission during these phases and the larger RVs imply a higher inclination for SDSS 1355+0856.

4 DISCUSSION

For the values of T_{eff} and $\log g$ determined from the co-added SDSS spectrum, the models of Panei et al. (2007) for He WDs give a mass of $M_1 = 0.46 \pm 0.01 M_\odot$, and those

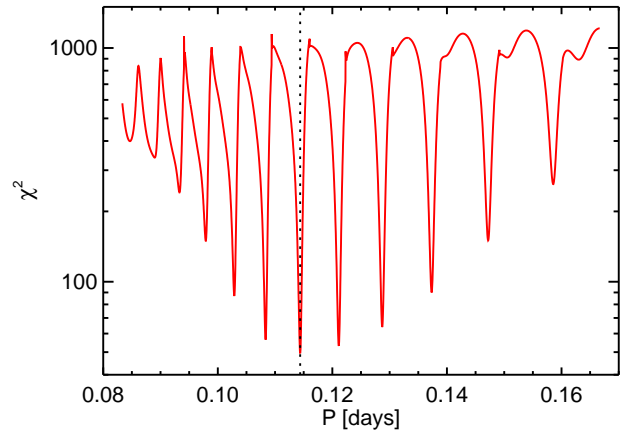
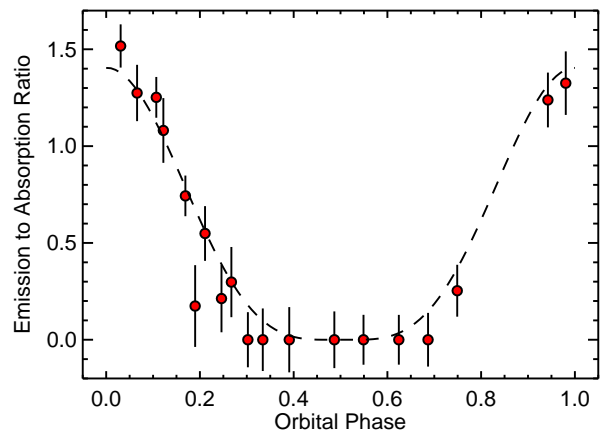
Table 2. Spectroscopic RVs for SDSS 1355+0856 from the MMT spectra

Spectrum	MJD (bar.)	v_a (km s $^{-1}$)	v_e (km s $^{-1}$)	F_e/F_a
MMT 0	55275.3824	-61.4 ± 18.1	69.2 ± 10.1	1.24 ± 0.14
MMT 1	55275.3868	-51.7 ± 21.7	7.4 ± 12.1	1.33 ± 0.16
MMT 2	55275.3925	3.8 ± 14.7	-64.9 ± 7.7	1.52 ± 0.11
MMT 3	55275.4012	44.2 ± 12.7	-188.7 ± 7.3	1.25 ± 0.11
MMT 4	55275.4083	39.1 ± 12.1	-243.9 ± 10.8	0.74 ± 0.10
MMT 5	55275.4447	-39.7 ± 15.9	...	0.00 ± 0.15
MMT 6	55275.4518	-42.6 ± 13.7	...	0.00 ± 0.13
MMT 7	55275.4604	-83.1 ± 14.2	...	0.00 ± 0.13
MMT 8	55275.4675	-95.6 ± 14.4	...	0.00 ± 0.14
MMT 9	55275.4747	-64.6 ± 15.3	187.1 ± 28.1	0.25 ± 0.13
MMT 10	55277.3577	39.6 ± 14.9	-299.0 ± 15.4	0.55 ± 0.14
MMT 11	55277.3642	-18.9 ± 20.5	-314.4 ± 25.6	0.30 ± 0.18
MMT 12	55277.3718	7.2 ± 15.6	...	0.00 ± 0.16
MMT 13	55277.3783	15.8 ± 16.2	...	0.00 ± 0.17
MMT 14	55277.4556	53.5 ± 17.9	-115.3 ± 10.0	1.27 ± 0.15
MMT 15	55277.4620	33.4 ± 18.2	-214.1 ± 13.4	1.08 ± 0.17
MMT 16	55277.4697	69.6 ± 24.7	-265.8 ± 54.1	0.17 ± 0.21
MMT 17	55277.4762	45.6 ± 19.5	-320.8 ± 39.4	0.21 ± 0.17
MMT 18	55277.4826	13.8 ± 14.1	...	0.00 ± 0.14

**Figure 5.** Orbital solution for SDSS 1355+0856. The red circles represent the RVs of the absorption component (WD), and the blue squares represent the RVs of the emission component in the spectra with $F_e/F_a > 0$. The value of γ_a (-23 km s $^{-1}$) has been marked with a horizontal dotted line.

of Holberg & Bergeron (2006) for C/O WDs give a slightly lower value of $M_1 = 0.43 \pm 0.01 M_\odot$. Since these values are both below the $\sim 0.48 M_\odot$ threshold for C ignition in a stellar core (Sweigart & Gross 1978), we conclude that the primary in the SDSS 1355+0856 system is most likely a hot He-core WD, and we adopt the mass given by the He-core models (however, see Prada Moroni & Straniero 2009, for the possibility that it might be a hybrid CO-He WD).

Even without considering the RVs measured for the line emission component, the mass of the companion is tightly constrained by the broadband SED of the system and the mass function of the WD primary derived from the absorption RVs. A quick comparison between the SED shown in Figure 3 and the theoretical models of Baraffe et al. (1998) rules out companions more massive than $\sim 0.1 M_\odot$, which would lead to noticeable excess flux in the IR, especially in the J , H , and K bands. More formally, we can set an

**Figure 6.** Periodogram for the orbital solution of SDSS 1355+0856, with indication of the best-fit period (0.11438 days).**Figure 7.** Behaviour of the F_e/F_a ratio in the MMT spectra of SDSS 1355+0856 as a function of orbital phase. The dashed line represents the model light curve discussed in Section 4.

upper limit on M_2 by requiring that the K -band flux predicted by the stellar models does not exceed the observed flux from UKIDSS by more than a factor 10. This generous tolerance should accommodate both the issues identified with theoretical low-mass stellar models (Casagrande et al. 2008; Kraus et al. 2011) and the uncertainties associated with the UKIDSS photometry (Leggett et al. 2011). By interpolating on the mass grid of the Baraffe et al. (1998) models, we determine a conservative upper limit of $0.097 M_\odot$ for M_2 . The mass function for the primary also puts constraints on the companion mass, requiring $M_2 \sin i = 0.098 \pm 0.016 M_\odot$, where the error bar reflects the observational uncertainty in the values of K_1 and M_1 . From these limits, we can conclude that the nondegenerate companion of SDSS 1355+0856 is a low-mass main sequence star with a mass between 0.083 and $0.097 M_\odot$, above the upper mass limit for brown dwarfs. The star should have a spectral type between M5 and M8 (Baraffe & Chabrier 1996), and be fully convective (Reiners & Basri 2009). Our failure to detect a significant offset between the RV curve of the WD and that of the line emission from the companion ($\Delta\gamma = -4 \pm 18 \text{ km s}^{-1}$ in our fit) does not allow us to put further constraints on the component masses using gravitational redshift, although this should be possible with data of higher quality (see discussion in Maxted et al. 1998, their Section 3.4, for the case of GD 448).

The RV curve that we have measured for the line emission provides an independent confirmation of our estimate for the companion mass. To interpret these RV measurements we need to account for the fact that the line emission does not originate from the entire surface of the companion, so the center of light for the line emission does not correspond to the center of mass for the star, but is shifted towards the WD. This means that the measured semiamplitude of the emission component, K_e , is only a lower limit to the true semiamplitude of the RV curve of the companion (K_2). This effect has been observed in other systems with hot WD primaries like GD 448 (Marsh & Duck 1996) and SDSS J212531.92–010745.9 (Nagel et al. 2006; Schuh et al. 2009), and is quite common in low mass X-ray binaries with NS primaries surrounded by an accretion disk (see MunozDarias et al. 2005, and references therein).

For a detached binary without an accretion disk, $K_e/K_2 = 1 - f(R_2/a_2)$, where a_2 is the orbital radius of the companion around the barycentre of the system, R_2 is the companion radius, and f is a dimensionless factor that depends on the extent of the irradiated area on the surface of the companion and on the orbital inclination of the binary (van Kerkwijk et al. 2011). In practice, the orbital inclination has a very small effect on the value of f for $i \gtrsim 50^\circ$ (MunozDarias et al. 2005; van Kerkwijk et al. 2011). We can estimate f by assuming the emission from the irradiated hemisphere is proportional to the incident flux from the primary. For an irradiating source at a large distance, the integral has an analytic solution at quadrature, and $f = 3\pi/16 = 0.59$, with higher values of f if the stars are closer together. For SDSS 1355+0856, we expect $R_2 \simeq 0.1 R_\odot$ (for a very low-mass M dwarf, Baraffe et al. 1998), $a \simeq 0.8 R_\odot$ (for a total mass of $\sim 0.59 M_\odot$), and thus $R_2/a = 1/8$. For that value, numerical integration yields $f = 0.66$ at quadrature, with a range of ± 0.02 for $1/10 < R_2/a < 1/6$. From Figure 7, one sees that such a

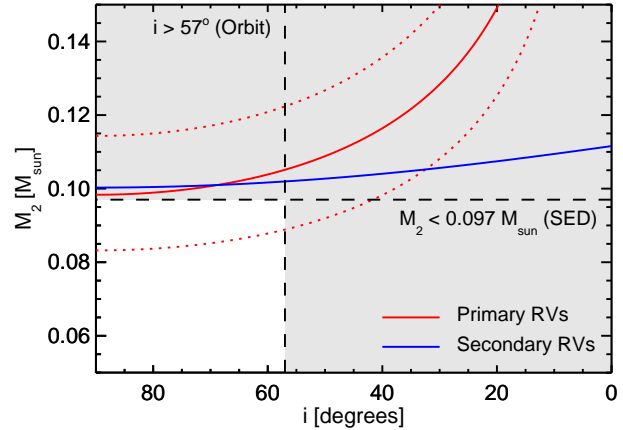


Figure 8. Observational constraints on M_2 and i for SDSS 1355+0856. The horizontal dashed line is the upper limit on M_2 derived from the SED (Figure 3). The vertical dashed line is the lower limit on i imposed by the measured value of K_e . The shaded regions above and to the right of these lines are forbidden by the data. The solid red line represents the constraint on $M_2 \sin i$ from the mass function of the primary, with the dotted red lines indicating standard 1σ uncertainties. The solid blue line represents the constraint from the measured value of K_e and the light curve model shown in Figure 7. The (rather large) uncertainty on this constraint is not shown.

model reproduces the flux ratio between the emission and absorption components in our spectral fits quite well. Trying different inclinations, we find that the absence of emission at phases 0.3–0.7 requires an inclination $i \gtrsim 52^\circ$ (for smaller inclination, the flux at phase 0.3 would exceed 20% of the maximum flux). After some algebra, we can write an expression for M_2 which depends strongly on measured parameters and weakly on R_2 and $\sin i$:

$$M_2 = \frac{M_1 K_1}{K_e + 2\pi f \sin i (R_2/P)}. \quad (1)$$

For the nominal values of M_1 , f , K_1 , and K_e , and $i = 90^\circ$, this yields $M_2 = 0.10 M_\odot$, which agrees quite nicely with our constraints from the mass function of the primary and the SED. Unfortunately, the error bars on K_1 and K_e are large enough that this method cannot refine our M_2 estimate any further, just confirm it. In any case, the measured value of K_e does put an upper limit on the orbital inclination,

$$\sin i \geq \frac{K_1 + K_e}{(2\pi G(M_1 + M_2)/P)^{1/3}}, \quad (2)$$

which translates to $i \geq 65 \pm 7^\circ$ (or a lower limit of 57°), with the uncertainty on the inclination angle is again dominated by the errors on K_1 and K_e . The limit is in line with our expectations from the mass constraints and the emission line lightcurve. We summarize our constraints on M_2 and i in Figure 8.

The picture that emerges from our analysis of SDSS 1355+0856 is that of a binary similar to GD 448 (Marsh & Duck 1996; Maxted et al. 1998). The two systems have almost identical component masses and period, but SDSS 1355+0856 has a somewhat higher inclination, leading to higher RVs and no detectable line emission between phases 0.25 and 0.75. The cooling age of the WD in SDSS 1355+0856 is $\sim 25 \text{ Myr}$ (Panei et al. 2007), about half the value for GD 448. This cooling time is much shorter

than both the thermal timescale of the companion (~ 5 Gyr) and the timescale for orbital decay due to gravitational wave emission (~ 2 Gyr). The system was probably born in the period gap of CVs, emerging from the CE phase with essentially the same period we can observe today. The possibility that SDSS 1355+0856 is instead crossing the period gap after a CV phase is unlikely, because (a) quiescent CVs usually have much cooler WDs (Townsend & Bildsten 2002) and (b) it is hard to imagine how mass transfer could have happened at a longer period with such a low mass companion. Since magnetic braking is inefficient for systems with fully convective secondaries (Schreiber & Gänsicke 2003; Zorotovic et al. 2011a), the future evolution of SDSS 1355+0856 will be dominated by gravitational wave radiation, but the system will still become semi-detached in less than a Hubble time, much like GD 448 (see Table 2 in Schreiber & Gänsicke 2003, and accompanying discussion). The low value of q (0.21) implies that mass transfer will be stable (Paczynski 1971; King et al. 1996). At this point, SDSS 1355+0856 will become one of the rare CVs with likely He-core WD primaries, possibly leading to a few exceptionally long classical nova events (Shen et al. 2009). The period and component masses of the system are such that it will contribute to future demographic constraints of CE evolution (see discussion in Zorotovic et al. 2011b), but we leave that analysis for further work.

ACKNOWLEDGMENTS

We wish to thank Detlev Koester for making his WD atmosphere models available to us. Balmer/Lyman lines in the Koester WD models were calculated with the modified Stark broadening profiles of Tremblay & Bergeron (2009), kindly made available by the authors. We are indebted to Scott Kleinman, who made his WD catalogue available to us in advance of publication. We are grateful to Eduardo Bravo, Avishay Gal-Yam, Shri Kulkarni, Dan Maoz, Thomas Matheson, Gijs Nelemans, Benny Trakhtenbrot, and Sharon Xuesong Wang for discussions.

Funding for the SDSS and SDSS-II has been provided by the Alfred P. Sloan Foundation, the Participating Institutions, the National Science Foundation, the U.S. Department of Energy, the National Aeronautics and Space Administration, the Japanese Monbukagakusho, the Max Planck Society, and the Higher Education Funding Council for England. The SDSS Web Site is <http://www.sdss.org/>. The SDSS is managed by the Astrophysical Research Consortium for the Participating Institutions. The Participating Institutions are the American Museum of Natural History, Astrophysical Institute Potsdam, University of Basel, University of Cambridge, Case Western Reserve University, University of Chicago, Drexel University, Fermilab, the Institute for Advanced Study, the Japan Participation Group, Johns Hopkins University, the Joint Institute for Nuclear Astrophysics, the Kavli Institute for Particle Astrophysics and Cosmology, the Korean Scientist Group, the Chinese Academy of Sciences (LAMOST), Los Alamos National Laboratory, the Max-Planck-Institute for Astronomy (MPIA), the Max-Planck-Institute for Astrophysics (MPA), New Mexico State University, Ohio State University, University of Pittsburgh, University of Portsmouth, Princeton

University, the United States Naval Observatory, and the University of Washington.

Facilities: MMT (Blue Channel Spectrograph); ARC 3.5m Telescope (Dual Imaging Spectrograph).

REFERENCES

- Badenes C., Maoz D., 2012, *ApJ*, 749, L11
 Badenes C., Mullally F., Thompson S. E., Lupton R. H., 2009, *ApJ*, 707, 971
 Baraffe I., Chabrier G., 1996, *ApJ*, 461, 1994
 Baraffe I., Chabrier G., Allard F., Hauschildt P. H., 1998, *A&A*, 412, 403
 Bickerton S., Badenes C., Hettinger T., Beers T., Huang S., 2012, *Proceedings of the IAU*, 7, 289
 Casagrande L., Flynn C., Bessell M., 2008, *MNRAS*, 389, 585
 Davis P. J., Kolb U., Knigge C., 2012, *MNRAS*, 419, 287
 De Marco O., Passy J.-C., Moe M., Herwig F., Mac Low M.-M., Paxton B., 2011, *MNRAS*, 411, 2277
 Finley D. S., Koester D., Basri G., 1997, *ApJ*, 488, 375
 Holberg J. B., Bergeron P., 2006, *AJ*, 132, 1221
 Ivanova N., Chaichenets S., 2011, *ApJ*, 731, L36
 Kilic M., Brown W. R., Allende Prieto C., Kenyon S. J., Panei J. A., 2010, *ApJ*, 716, 122
 King A. R., Frank J., Kolb U., Ritter H., 1996, *ApJ*, 467, 761
 Kleinman S. J., Nitta A., Koester D., 2009, *Journal of Physics: Conference Series*, 172, 012020
 Koester D., *MmSAI*, 2010, 81, 921
 Kraus A. L., Tucker R. A., Thompson M. I., Craine E. R., Hillenbrand L. A., 2011, *ApJ*, 728, 48
 Lawrence A., et al., 2007, *MNRAS*, 379, 1599
 Leggett S. K., Lodieu N., Tremblay P.-E., Bergeron P., Nitta A., 2011, *ApJ*, 735, 62
 Maoz D., Badenes C., Bickerton S. J., 2012, *ApJ*, 751, 143
 Marsh T. R., Duck S. R., 1996, *MNRAS*, 278, 565
 Massey P., Strobel K., Barnes J. V., Anderson E., 1988, *ApJ*, 328, 315
 Maxted P. F. L., Marsh T. R., Moran C., Dhillon V. S., Hilditch R. W., 1998, *MNRAS*, 300, 1225
 Morrissey P., et al., 2007, *ApJS*, 173, 682
 Mullally F., Badenes C., Thompson S. E., Lupton R., 2009, *ApJ*, 707, L51
 MunozDarias T., Casares J., MartinezPais I. G., 2005, *ApJ*, 635, 502
 Nagel T., Schuh S., Kusterer D.-J., Stahn T., Hügelmeier S. D., Dreizler S., Gänsicke B. T., Schreiber M. R., 2006, *A&A*, 448, L25
 Paczynski B., 1971, *ARA&A*, 9, 183
 —, 1976, *Structure and Evolution of Close Binary Systems; Proceedings of the Symposium*
 Panei J. A., Althaus L. G., Chen X., Han Z., 2007, *MNRAS*, 382, 779
 Prada Moroni P. G., Straniero O., 2009, *A&A*, 507, 1575
 Rebassa-Mansergas A., Gänsicke B. T., Schreiber M. R., Koester D., Rodríguez-Gil P., 2010, *MNRAS*, 402, 620
 Rebassa-Mansergas A., Nebot Gómez-Morán A., Schreiber M. R., Gänsicke B. T., Schwöpe A., Gallardo J., Koester D., 2012, *MNRAS*, 419, 806
 Reiners A., Basri G., 2009, *A&A*, 496, 787

- Ricker P. M., Taam R. E., 2012, *ApJ*, 746, 74
- Schreiber M. R., Gänsicke B. T., 2003, *A&A*, 406, 305
- Schuh S., Bееck B., Nagel T., 2009, *Journal of Physics: Conference Series*, 172, 012065
- Shen K. J., Idan I., Bildsten L., 2009, *ApJ*, 705, 693
- Sweigart A. V., Gross P. G., 1978, *ApJS*, 36, 405
- Taam R. E., Sandquist E. L., 2000, *ARA&A*, 38, 113
- Townsley D. M., Bildsten L., 2002, *ApJ*, 565, L35
- Tremblay P.-E., Bergeron P., 2009, *ApJ*, 696, 1755
- van Kerkwijk M. H., Breton R. P., Kulkarni S. R., 2011, *ApJ*, 728, 95
- Webbink R. F., 2006, *American Astronomical Society Meeting 208*, 38
- Zorotovic M., Schreiber M. R., Gänsicke B. T., 2011a, *A&A*, 536, A42
- Zorotovic M., Schreiber M. R., Gänsicke B. T., Nebot Gómez-Morán A., 2010, *A&A*, 520, A86
- Zorotovic M., et al., 2011b, *A&A*, 536, L3